 CMES, vol.14, no.3, pp.181-198, 2006

# SPH in a Total Lagrangian Formalism

**Rade Vignjevic[1], Juan R. Reveles[1], James Campbell[1]**

**Abstract:** To correct some of the main shortcomings of conventional SPH, a version of this method based on the Total Lagrangian formalism, T. Rabczuk, T. Belytschko and S. Xiao (2004), is developed. The resulting scheme removes the spatial discretisation instability inherent in conventional SPH, J. Monaghan (1992).
The Total Lagrangian framework is combined with the mixed correction which ensures linear completeness and compliance with the patch test, R. Vignjevic, J. Campbell, L. Libersky (2000). The mixed correction utilizes Shepard Functions in combination with a correction to derivative approximations.
Incompleteness of the kernel support combined with the lack of consistency of the kernel interpolation in conventional SPH results in fuzzy boundaries. In corrected SPH, the domain boundaries and field variables at boundaries are approximated with the default accuracy of the method.
Additionally, these corrections are introduced into the Total Lagrangian SPH and compared to the conventional SPH and to a number of selected corrected variants, G. Johnson, R. Stryk, S. Beissel (1996), J. Bonet, S. Kulasegaram (2002), and P. Randles, L. Libersky (1996). The resulting Total Lagrangian SPH scheme not only ensures fist order consistency but also alleviates the particle deficiency (kernel support incompleteness) problem. Furthermore a number of improvements to the kernel derivative approximation are proposed.
To illustrate the performance of the Total Lagrangian SPH and the mixed correction, four numerical examples ranging from simple 1D dynamic elasticity to 3D real engineering problems are also provided.

**keyword:** Stable particle methods, Total Lagrangian SPH, Impact , Corrected SPH.

[1] Cranfield University, Cranfield, Bedford, MK43 0AL, UK. email: v.rade@cranfield.ac.uk

## 1 Introduction

It is well known that the conventional SPH method initially proposed by L. Lucy (1977) and Gingold and Monaghan (1977) has a number of shortcomings including inconsistency (not even zero order consistent for arbitrary distribution of particles), rank deficiency , J. Sweegle, D. Hicks, S. Attaway (1995), and a spatial discretisation related instability, T. Rabczuk, T. Belytschko and S. Xiao (2004) and J. Sweegle, D. Hicks, S. Attaway (1995) often called tensile instability.

The recent improvements of the conventional SPH method which have given the method first order consistency, R. Vignjevic, J. Campbell, L. Libersky (2000) and , J. Bonet, S. Kulasegaram (2002), have been achieved by modifying the properties of the kernel function itself, see W. Liu, Y. Chen (1995) and W. Liu, S. Jun, J. Adee, T. Belytschko (1995) or by applying corrections to the interpolation integral, R. Vignjevic, J. Campbell, L. Libersky (2000), J. Bonet, S. Kulasegaram (2002). The outstanding problems with tensile instability combined with the lack of rigorous treatment of boundary conditions still hamper the full exploitation of the method.

A number of solutions to the tensile instability problem have been proposed, including non-collocational SPH (where stress and velocity fields are discretised at different locations R. Vignjevic, J. Campbell, L. Libersky (2000), C. Dyka, R. Ingel (1995)) and Lagrangian kernel based interpolation T. Rabczuk, T. Belytschko and S. Xiao (2004). In this paper the interest is focused on Lagrangian kernels in a total Lagrangian framework for SPH and the different types of corrections necessary for first order consistency.

A comprehensive overview of current correction techniques with the SPH discretised conservation equations in a total Lagrangian framework is given. Additionally, the effects of the normalisation of the kernel and accuracy of approximations of the derivatives are considered. An alternative to the approach considered in this paper which does not have stability problems related to

the spatial discretisation is the Meshless Local Petrov-Galerkin (MLPG) method, Atluri, S.N (1998, 2004) and Han (2005) but this alternative requires additional effort and care in the treatment of boundary conditions.

A number of numerical examples ranging from simple 1D dynamic elasticity to 3D real engineering problems are also provided to illustrate the performance of the Total Lagrangian SPH and the mixed correction.

## 2 Conventional SPH

The SPH method is based on the convolution principle or interpolant integral. Thus, any exact physical field (scalar, vector or tensor) $\psi(\tilde{\mathbf{x}},t)$ which depends on position $\tilde{\mathbf{x}}$ and on time $t$ can be approximated by its smoothed value $\langle\psi(\tilde{\mathbf{x}},t)\rangle$ given by

$$<\psi(\tilde{\mathbf{x}},t)>=\int_{D_hW}\psi(\mathbf{s},t).W(|\tilde{\mathbf{x}}-\mathbf{s}|,h).\left(\frac{\rho(\mathbf{s},t).ds}{\rho(\mathbf{s},t)}\right) \quad (1)$$

Where: $W(|\tilde{\mathbf{x}}-\mathbf{s}|,h)$ is the kernel function and, $h$ is a geometrical parameter which defines size of the kernel support, ρis the density and $D_hW$ is the compact support of the kernel.

$$\begin{aligned} D_hW &= \left\{\tilde{\mathbf{x}}-\mathbf{s}/\,|\tilde{\mathbf{x}}-\mathbf{s}|\in\Re^N, W(|\tilde{\mathbf{x}}-\mathbf{s}|,h)\in\Re^*\right\} \\ &= \{\vec{x}-s/\,|\vec{x}-s|\in\Re^N, |\vec{x}-s|\in[-C.h,+C.h]\} \end{aligned} \quad (2)$$

Where: $C$ is a constant

The second equality is only valid for kernels with symmetric support.

The kernel $W(|\tilde{\mathbf{x}}-\mathbf{s}|,h)$ should have the following properties:

$$\int_{D_hW} W(|\tilde{\mathbf{x}}-\mathbf{s}|,h).ds=1 \quad (3)$$

$$W(|\tilde{\mathbf{x}}-\mathbf{s}|,h)\overset{h\to 0}{\longrightarrow}\delta_z \quad (4)$$

Where: $\delta_z$is Dirac delta function.

For numerical applications the domain of integration has to be discretised, in that case Eq. (1) is approximated by:

$$<\psi(\tilde{\mathbf{x}}_I)>\approx\sum_{J\in Ni}\psi(\tilde{\mathbf{x}}_J)\cdot W(|\tilde{\mathbf{x}}_I-\tilde{\mathbf{x}}_J|,h)\cdot\frac{m_J}{\rho(\tilde{\mathbf{x}}_J)} \quad (5)$$

Where: $m_J$ is the mass associated with particle $J$, $N_i$ is the set of particles interacting with $I^{th}$ particle and $ds_J = m_J/\rho(\tilde{\mathbf{x}}_J)\cdot$,$S=\{J\in N/-C.h\le\tilde{\mathbf{x}}_I-\tilde{\mathbf{x}}_J\le C.h\}$

The interpolation defined by Eq. (5) is not even zero order consistent for irregular distribution of particles.

The spatial derivative of ψ is approximated as:

$$\begin{aligned} <\frac{\partial\psi(\tilde{\mathbf{x}}_I)}{\partial\mathbf{x}}> &\approx\sum_{J\in N_i}\psi(\tilde{\mathbf{x}}_J).\frac{\partial W}{\partial\vec{x}_J}(\tilde{\mathbf{x}}_I-\tilde{\mathbf{x}}_J,h).\frac{m_J}{\rho(\tilde{\mathbf{x}}_J)} \\ &=\sum_{J\in N_i}\psi(\tilde{\mathbf{x}}_J).W_{IJ}\frac{m_J}{\rho_J} \end{aligned} \quad (6)$$

This derivative approximation is inaccurate even for constant and linear fields.

Using approximations defined by Eqs. (5) and (6) it is possible to derive several forms of the discretised equations of conservation, for details see J. Monaghan (1992). One of the forms is given below.

- Conservation of mass

$$\dot{\rho}=-\rho\,\nabla\cdot\tilde{\mathbf{v}} \quad\Rightarrow\quad \dot{\rho}_I=\rho_I\sum_{J\in S}\frac{m_J}{\rho_J}(\tilde{\mathbf{v}}_J-\tilde{\mathbf{v}}_I)\cdot\nabla\mathbf{W}_{IJ} \quad (7)$$

- Conservation of momentum

$$\dot{\mathbf{v}}=\frac{1}{\rho}\nabla\cdot\overline{\overline{\sigma}} \qquad \Rightarrow\dot{\mathbf{v}}_I=\sum_{J\in S}m_j\left(\frac{\overline{\overline{\sigma}}_I}{\rho_I^2}+\frac{\overline{\overline{\sigma}}_J}{\rho_J^2}\right)\nabla\mathbf{W}_{IJ} \quad (8)$$

- Conservation of energy

$$\begin{aligned} \dot{e} &= \frac{1}{\rho}\nabla\cdot\left(\overline{\overline{\sigma}}\tilde{\mathbf{v}}\right)-\tilde{\mathbf{v}}\cdot\dot{\tilde{\mathbf{v}}} \\ &\Rightarrow\dot{e}_I=-\frac{\overline{\overline{\sigma}}_I}{\rho_I^2}:\sum_{J\in S}\;m_J\;(\tilde{\mathbf{v}}_J-\tilde{\mathbf{v}}_I)\nabla\,\mathbf{W}_{IJ} \end{aligned} \quad (9)$$

A common characteristic of these equations is that conservation of linear momentum and energy is satisfied locally. This is in part due to the fact that the kernels used in the interpolation are symmetric.

## 3 Overview of correction and normalization techniques.

Several approaches have been developed for improving the consistency of the conventional SPH method, in this section we refer to three methods termed normalization, correction and normalization and correction. These

terms are used interchangeably in literature but we adhere to the following convention: normalization refers to the improvement which gives the zero order consistency to the interpolation method while correction refers to the improvement of the approximation of the gradient and gives the interpolation scheme first order consistency. The term normalized-corrected refers to the corrected gradient approximation combined with normalised smoothing function.

### 3.1 Kernel normalization.

Normalization or kernel correction is aimed at making the interpolation scheme $0^{th}$ order consistent by removing the effects of the kernel domain incompleteness and irregularity in locations of sampling points (particles). The approximation of fields using a Normalised Corrected SPH (NCSPH) interpolation has been published, R. Vignjevic, J. Campbell, L. Libersky (2000), P. Randles, L. Libersky (1996), J. Bonet, S. Kulasegaram (2000). Some authors have chosen to use properties of the integrals of motion (linear and angular momentum) to derive Normalisation and Gradient Correction for kernel interpolation, see J. Bonet, S. Kulasegaram (2000). This approach lacks generality and does not provide the insight into the origin and the nature of the problem. A full derivation of the correction proposed by Vignjevic, Campbell and Libersky (2000), is given below. The derivation is based on Noether's theorem, I. Gelfand, S. Formin (1963), i.e. the homogeneity and isotropy of space. The mixed interpolation correction ensures that homogeneity and isotropy of space are preserved in the process of spatial discretisation. Consequently, conservation of linear and angular momentum is ensured.

The normalization of the smoothing function guarantees that the condition given in Eq. (10) is satisfied over the entire domain.

$$\sum_{J\in S} W\left(\tilde{\mathbf{x}}-\tilde{\mathbf{x}}_J,h\right)\frac{m_J}{\rho\left(\vec{\mathbf{x}}_J\right)}=1 \tag{10}$$

A normalised smoothing function which correctly reproduces a constant field and satisfies the above condition is known as Shepard function and is given by:

$$\tilde{W}\left(\tilde{\mathbf{x}}_{-}\tilde{\mathbf{x}}_J,h\right)=\frac{W\left(\tilde{\mathbf{x}}_{-}\tilde{\mathbf{x}}_J,h\right)}{\sum\limits_{J\in S}\frac{m_J}{\rho_J}W\left(\tilde{\mathbf{x}}_{-}\tilde{\mathbf{x}}_J,h\right)} \tag{11}$$

The derivation of this form starts with the assumption that an interpolation technique should not affect homogeneity of space. A way of demonstrating this is to prove that the discretised solution space itself is independent of a translation of the coordinate axes. In order to express this statement mathematically one can start by writing the general expression for the SPH interpolation of a vector field:

$$\left\langle\tilde{\mathbf{F}}\left(\tilde{\mathbf{x}}\right)\right\rangle\big|_{\tilde{\mathbf{x}}=\tilde{\mathbf{x}}_I}=\sum_{J\in S}\frac{m_J}{\rho_J}\tilde{\mathbf{F}}\left(\tilde{\mathbf{x}}_J\right)W\left(\tilde{\mathbf{x}}_I-\tilde{\mathbf{x}}_J,h\right) \tag{12}$$

If the field to be interpolated is the solution space then $\tilde{\mathbf{F}}=\tilde{\mathbf{x}}$ and Eq. (12) becomes:

$$\left\langle\tilde{\mathbf{x}}\right\rangle\big|_{\tilde{\mathbf{x}}=\tilde{\mathbf{x}}_I}=\sum_{J\in S}\frac{m_J}{\rho_J}\tilde{\mathbf{x}}_J W\left(\tilde{\mathbf{x}}_I-\tilde{\mathbf{x}}_J,h\right) \tag{13}$$

In a different, translated coordinate system, this equation is:

$$\left\langle\tilde{\mathbf{x}}'\right\rangle\big|_{\tilde{\mathbf{x}}'=\tilde{\mathbf{x}}'_I}=\sum_{J\in S}\frac{m_J}{\rho_J}\tilde{\mathbf{x}}'_J W\left(\tilde{\mathbf{x}}'_I-\tilde{\mathbf{x}}'_J,h\right) \tag{14}$$

Where $\tilde{\mathbf{x}'}$ is the coordinate vector in the new coordinate system. If the translation vector by which the origin of the coordinate system was moved is defined as $\Delta\tilde{\mathbf{x}}$ then the relationship between $\tilde{\mathbf{x}}$ and $\tilde{\mathbf{x}'}$is:

$$\tilde{\mathbf{x}'}=\tilde{\mathbf{x}}-\Delta\tilde{\mathbf{x}} \tag{15}$$

If the interpolated coordinates of a point are independent of the translation of coordinate axes then the following should hold:

$$\left\langle\tilde{\mathbf{x}}'\right\rangle=\left\langle\tilde{\mathbf{x}}\right\rangle-\Delta\tilde{\mathbf{x}} \tag{16}$$

By substituting Eq. (16) into Eq. (15) for both $\tilde{\mathbf{x}}_I$and $\tilde{\mathbf{x}}_J$ one obtains:

$$\left\langle\tilde{\mathbf{x}}'\right\rangle=\sum_{J\in S}\frac{m_J}{\rho_J}\tilde{\mathbf{x}}_J W\left(\tilde{\mathbf{x}}_I-\tilde{\mathbf{x}}_J,h\right)--\Delta\tilde{\mathbf{x}}\sum_{J\in S}\frac{m_J}{\rho_J}W\left(\tilde{\mathbf{x}}_I-\tilde{\mathbf{x}}_J,h\right) \tag{17}$$

or

$$\left\langle\tilde{\mathbf{x}}'\right\rangle=\left\langle\tilde{\mathbf{x}}\right\rangle-\Delta\tilde{\mathbf{x}}\sum_{J\in S}\frac{m_J}{\rho_J}W\left(\tilde{\mathbf{x}}_I-\tilde{\mathbf{x}}_J,h\right) \tag{18}$$

By comparison of Eq. (18) and Eq. (16) it is clear that the discretised space will only be homogeneous if kernel function satisfies condition given in Eq. (12).

The form of the kernel function that satisfies this condition can be obtained by dividing Eq. (17) by $\sum_{J\in S}\frac{m_J}{\rho_J}W(\tilde{\mathbf{x}}_I-\tilde{\mathbf{x}}_J,h)$, i.e:

$$\begin{aligned}\left\langle\tilde{\mathbf{x}}'\right\rangle &= \sum_{J\in S}\frac{m_J}{\rho_J}\tilde{\mathbf{x}}_J\frac{W(\tilde{\mathbf{x}}_I-\tilde{\mathbf{x}}_J,h)}{\sum_j\frac{m_j}{\rho_j}W(\tilde{\mathbf{x}}_I-\tilde{\mathbf{x}}_J,h)}-\Delta\tilde{\mathbf{x}}\\ &= \sum_{J\in S}\frac{m_J}{\rho_J}\tilde{\mathbf{x}}_J\tilde{W}(\tilde{\mathbf{x}}_I-\tilde{\mathbf{x}}_J,h)-\Delta\tilde{\mathbf{x}}\end{aligned} \tag{19}$$

Where: $\tilde{W}$ is the Shepard function.

### 3.2 Correction of the derivatives.

A simple correction technique involves modification of the kernel gradient by introducing a correction matrix denoted by **L,** J. Bonet, S. Kulasegaram (2002), or **B**, P. Randles, L. Libersky (1996), in literature. This corrections are aimed at restoring $1^{st}$ order consistency.

There are several ways in which this correction can be obtained, two derivations are presented here.

First let's start by considering a function $\psi(x')$ in a 1-D space which is assumed to be sufficiently smooth in the domain that contains $x$. Performing the Taylor series expansion for $\psi(x')$ in the vicinity of $x$ yields:

$$\psi(x')=\psi(x)+(x'-x)\frac{\partial\psi(x)}{\partial x}\frac{(x'-x)^2}{2}\frac{\partial^2\psi(x)}{\partial x^2}+... \tag{20}$$

Multiplying both sides of the equation by a smoothing function $W$and integrating over the sub-domain $S$:

$$\begin{aligned}\int_S\psi(x')W(x')dx' &= \psi(x)\int_S W(x')dx'\\ &+\frac{\partial\psi(x)}{\partial x}\int_S(x'-x)W(x')dx'\\ &+\frac{\partial^2\psi(x)}{\partial x^2}\int_S\frac{(x'-x)^2}{2}W(x')dx'+...\end{aligned} \tag{21}$$

In order to approximate the derivative of the function $\psi$ rather than the function $\psi$ itself, the function $W$ can be replaced by the derivative of the function $W$in the above expression as follows:

$$\begin{aligned}\int_S\psi(x')\frac{\partial W(x')}{\partial x}dx' &= \psi(x)\int_S\frac{\partial W(x')}{\partial x}dx'\\ &+\frac{\partial\psi(x)}{\partial x}\int_S(x'-x)\frac{\partial W(x')}{\partial x}dx'\\ &+\frac{\partial^2\psi(x)}{\partial x^2}\int_S\frac{(x'-x)^2}{2}\frac{\partial W(x')}{\partial x}dx'+...\end{aligned} \tag{22}$$

From where the corrected expression for the first derivative, neglecting higher order terms, is given by:

$$\frac{\partial\psi(x)}{\partial x}=\frac{\int_S(\psi(x')-\psi(x))\frac{\partial W(x')}{\partial x}dx'}{\int_S(x'-x)\frac{\partial W(x')}{\partial x}dx'} \tag{23}$$

A discrete form of the expression above is given by:

$$\left\langle\frac{\partial\psi(x_I)}{\partial x}\right\rangle=\frac{\sum_{J\in S}\frac{m_J}{\rho_J}(\psi_J-\psi_I)\frac{\partial W_{IJ}}{\partial x}}{\sum_{J\in S}\frac{m_J}{\rho_J}(x_J-x_I)\frac{\partial W_{IJ}}{\partial x}} \tag{24}$$

Where the derivatives are with respect to the $x'$ and $W_{IJ}=W(x_I-x_J,h)$.

The above is the discretised expression for the gradient correction of a function $\psi(x')$; the numerator is the kernel approximation for the first derivative of a function and the denominator acts as the correction factor. It is easy to extend the procedure to 2D and 3D.

From the above expression it is not entirely clear how the $1^{st}$ order consistency of the method gets restored. An alternative approach to derivation of the correction of the derivatives may provide additional insight. To this end one can consider approximation of a linear function based on SPH framework.

Let's consider a linear velocity field in a 1-D defined as:

$$v=\mathrm{a}+\mathrm{bx} \tag{25}$$

Where: a and b are constants. The approximation of gradient of this velocity field $L$ based on corrected SPH is:

$$L=\frac{\partial v}{\partial x}=\left(-\sum_{J\in S}\frac{m_J}{\rho_J}(v_J-v_I)\frac{\partial W_{IJ}}{\partial x}.B\right) \tag{26}$$

Hence, $B$ can be readily obtained as:

$$B = \left( -\sum_{J \in S} \frac{m_J}{\rho_J} (x_J - x_I) \nabla W_{IJ} \right)^{-1} \tag{27}$$

Correction factor B is equivalent to the expression in the denominator in Eq. (24). The above derivation has been extended to 3-D by Randles and Libersky (1996), the tensor form of the correction can be written as follows:

$$\mathbf{B} = \left( -\sum_{J \in S} \frac{m_J}{\rho_J} (\tilde{\mathbf{x}}_J - \tilde{\mathbf{x}}_I) \otimes \nabla W_{IJ} \right)^{-1} \tag{28}$$

or in index notation:

$$\mathrm{B}_{\alpha\beta} = \left( -\sum_{J \in S} \frac{m_J}{\rho_J} (x_J^\alpha - x_I^\alpha) \frac{\partial W}{\partial x^\beta} \right)^{-1} \tag{29}$$

### *3.3 Normalisation of the kernel with correction of the derivatives.*

Another possible correction technique is achieved by combining the normalized smoothing function with the correction of the derivatives, R. Vignjevic, J. Campbell, L. Libersky (2000), J. Bonet, S. Kulasegaram (2002). In this particular case, one starts with the normalized smoothing function (the Sheppard function) and the assumption that an interpolation technique should not affect isotropy of space. One way of demonstrating this is to prove that the interpolation is independent of a rotation of the coordinate axes. The same holds for the SPH approximation. The change in coordinates due to a rotation of the coordinate axes is:

$$\tilde{\mathbf{x}}' = \mathbf{C}\tilde{\mathbf{x}} \tag{30}$$

Where: $\mathbf{C}$ is the rotation matrix. For small rotations this can also be written as:

$$\tilde{\mathbf{x}}' = \tilde{\mathbf{x}} - \Delta\vec{\phi} \times \tilde{\mathbf{x}} \tag{31}$$

Where $\Delta\vec{\phi}$ is the rotation vector.

If one wants to ensure that the SPH approximation does maintain the fact that space is isotropic then the approximation has to satisfy the following condition:

$$\left\langle \tilde{\mathbf{x}}' \right\rangle \equiv \langle \mathbf{C}\tilde{\mathbf{x}} \rangle = \mathbf{C} \langle \tilde{\mathbf{x}} \rangle \tag{32}$$

or

$$\langle \mathbf{C} \rangle = \mathbf{C} \tag{33}$$

This means that the rotation matrix has to be approximated exactly.

In order to develop this equation one can start by rewriting

$$\begin{aligned} \tilde{\mathbf{x}}' &= \tilde{\mathbf{x}} - \Delta\vec{\phi} \times \tilde{\mathbf{x}} \\ &= \tilde{\mathbf{x}} - \nabla \left( \Delta\vec{\phi} \times \tilde{\mathbf{x}} \right) \cdot \tilde{\mathbf{x}} \\ &= \tilde{\mathbf{x}} - \phi^x \tilde{\mathbf{x}} \\ &= (\mathbf{I} - \phi^{\mathbf{x}}) \tilde{\mathbf{x}} \end{aligned} \tag{34}$$

Where $\Delta\phi^x$ is a skew-symmetric matrix:

$$\Delta\phi^x = \begin{bmatrix} 0 & -\Delta\phi_z & \Delta\phi_y \\ \Delta\phi_z & 0 & -\Delta\phi_x \\ -\Delta\phi_y & \Delta\phi_x & 0 \end{bmatrix} \tag{35}$$

Consequently the rotation matrix, for small rotations, is given by:

$$\mathbf{C} = \mathbf{I} - \phi^{\mathbf{x}} \tag{36}$$

The approximation of the rotated coordinates is:

$$\left\langle \tilde{\mathbf{x}}' \right\rangle \equiv \langle \mathbf{C}\tilde{\mathbf{x}} \rangle = \langle \mathbf{C} \rangle \langle \tilde{\mathbf{x}} \rangle = \langle \mathbf{I} - \phi^x \rangle \langle \tilde{\mathbf{x}} \rangle \tag{37}$$

The condition given in Eq. (33) can be rewritten as:

$$\mathbf{I} - \phi^x = \langle \mathbf{I} - \phi^x \rangle \tag{38}$$

or

$$\phi^x = \langle \phi^x \rangle \tag{39}$$

Expanding this expression leads to:

$$\begin{aligned} \langle \phi^x \rangle &= \sum_{J \in S} \frac{m_J}{\rho_J} \Delta\vec{\phi} \times \tilde{\mathbf{x}}_J \otimes \nabla \tilde{W} (\tilde{\mathbf{x}}_I - \tilde{\mathbf{x}}_J, h) \\ &= \sum_{J \in S} \frac{m_J}{\rho_J} (\phi^x \tilde{\mathbf{x}}_J) \otimes \nabla \tilde{W} (\tilde{\mathbf{x}}_I - \tilde{\mathbf{x}}_J, h) \\ &= \phi^x \sum_{J \in S} \frac{m_J}{\rho_J} \tilde{\mathbf{x}}_J \otimes \nabla \tilde{W} (\tilde{\mathbf{x}}_I - \tilde{\mathbf{x}}_J, h) \end{aligned} \tag{40}$$

Therefore, to preserve space isotropy, i.e. $\phi^x = \langle \phi^x \rangle$ the following condition has to be satisfied.

$$\sum_{J \in S} \frac{m_J}{\rho_J} \tilde{\mathbf{x}}_J \otimes \nabla \tilde{W} (\tilde{\mathbf{x}}_I - \tilde{\mathbf{x}}_J, h) = \mathbf{I} \tag{41}$$

The approximation of the derivative which satisfies this condition can be obtained by multiplying Eq. (40) by $\left[\sum_{J\in S}\frac{m_J}{\rho_J}\tilde{\mathbf{x}}_J\otimes\nabla\tilde{W}\left(\tilde{\mathbf{x}}_I-\tilde{\mathbf{x}}_J,h\right)\right]^{-1}$:

$$\begin{aligned}\langle\phi^x\rangle=\phi^x=&\sum_{J\in S}\frac{m_J}{\rho_J}\left(\phi^x\tilde{\mathbf{x}}_J\right)\otimes\nabla\tilde{W}\left(\tilde{\mathbf{x}}_I-\tilde{\mathbf{x}}_J,h\right)\times\\&\left[\sum_{J\in S}\frac{m_J}{\rho_J}\tilde{\mathbf{x}}\otimes\nabla\tilde{W}\left(\tilde{\mathbf{x}}_I-\tilde{\mathbf{x}}_J,h\right)\right]^{-1}\\=&\sum_{J\in S}\frac{m_J}{\rho_J}\left(\phi^x\tilde{\mathbf{x}}_J\right)\otimes\nabla\tilde{W}\left(\tilde{\mathbf{x}}_I-\tilde{\mathbf{x}}_J,h\right)\mathbf{B}\\=&\sum_{J\in S}\frac{m_J}{\rho_J}\left(\phi^x\tilde{\mathbf{x}}_J\right)\otimes\tilde{\nabla}\tilde{W}\left(\tilde{\mathbf{x}}_I-\tilde{\mathbf{x}}_J,h\right)\end{aligned}\tag{42}$$

The forms of the normalised kernel function and the approximation of the first order derivatives which provide first order consistency are given in **Table 1**.

Using the NCSPH approximations the conventional SPH conservation equations assume the following form:

$$\langle\dot{\rho}_I\rangle=\rho_I\sum_{J\in S}\frac{m_J}{\rho_J}\left(\tilde{\mathbf{v}}_J-\tilde{\mathbf{v}}_I\right)\cdot\tilde{\nabla}\tilde{\mathbf{W}}_{IJ}\tag{43}$$

$$\left\langle\dot{\tilde{\mathbf{v}}}_I\right\rangle=\sum_{J\in S}m_j\left(\frac{\bar{\bar{\sigma}}_i}{\rho_i^2}+\frac{\bar{\bar{\sigma}}_j}{\rho_j^2}\right)\tilde{\nabla}\tilde{\mathbf{W}}_{IJ}\tag{44}$$

$$\langle\dot{e}_I\rangle=-\frac{\sigma_i}{\rho_i^2}:\sum_{J\in S}m_J\left(\tilde{\mathbf{v}}_J-\tilde{\mathbf{v}}_I\right)\otimes\tilde{\nabla}\tilde{\mathbf{W}}_{IJ}\tag{45}$$

An alternative approach to normalised-corrected SPH assumes that the denominator in the normalised smoothing function $\tilde{W}_{IJ}$ given in Table 1 remains constant. In this case, the derivative of the normalised function is expressed by:

$$\nabla\tilde{W}_{ij}=\frac{1}{C}\nabla W_{ij}\tag{46}$$

Where: $C$ is simply

$$\sum_{J=1}^{nnbr}\frac{m_J}{\rho_J}W\left(\tilde{\mathbf{x}}_I-\tilde{\mathbf{x}}_J,h\right)\tag{47}$$

for the normalised corrected form of Eq. (46) a correction term $\mathbf{B}$ would have to be introduced such that

$$\tilde{\nabla}\tilde{W}_{ij}=\frac{1}{C}\nabla W_{ij}\mathbf{B}\tag{48}$$

**Table 1** : Corrected forms of the kernel function and its gradient

| | Space Homogeneity |
|---|---|
| Condition | $\sum_{Js\varepsilon s}\frac{m_J}{\rho_J}W(\tilde{\mathbf{x}}_I-\tilde{\mathbf{x}}_J,h)=I$ |
| Normalised-Corrected | $\tilde{W}_{IJ}=\frac{W(\tilde{\mathbf{x}}_I-\tilde{\mathbf{x}}_J,h)}{\sum_{Js\varepsilon s}\frac{m_J}{\rho_J}W(\tilde{\mathbf{x}}_I-\tilde{\mathbf{x}}_J,h)}$ |
| | Space Isotropy |
| Condition | $\sum_{Js\varepsilon s}\frac{m_J}{\rho_J}\tilde{\mathbf{x}}_J\otimes\nabla W(\tilde{\mathbf{x}}_I-\tilde{\mathbf{x}}_J,h)=I$ |
| Normalised-Corrected | $\tilde{\nabla}\tilde{\mathbf{W}}_{IJ}=\nabla\tilde{\mathbf{W}}_{IJ}\left(\sum_{Js\varepsilon s}\frac{m_J}{\rho_J}\tilde{\mathbf{x}}_J\otimes\nabla\tilde{\mathbf{W}}_{IJ}\right)^{-1}$ |

or, in index notation:

$$\tilde{\nabla}\tilde{W}_\alpha=\frac{1}{C}\frac{\partial W}{\partial x_\beta}B_{\beta\alpha}\tag{49}$$

Eq. (49) provides a simplified form of Eq. (10). which restores first order consistency to the conventional SPH.

One can see that generally $W_{CNSPH}(x,x-s,h)\neq W_{CNSPH}(s,s-x,h)$, i.e. the kernel function is no longer symmetric this should be reflected in the form of the semidiscretised conservation equations based on this type of interpolation.

## 4 Total Lagrangian formalism for SPH.

### *4.1 Conservation Equations in the Total Lagrangian formalism.*

To describe motion of continuum equation of conservation of mass momentum and energy and the constitutive laws have o be integrated.

Usually, when using total Lagrangian approach the initial state of the domain of interest is regarded as the reference state. In this analysis the same assumption was made, hence the conservation and constitutive equations will be expressed in terms of material coordinates.

This implies that when the Spatial and Material reference frames are coincident the mapping that transforms material into spatial coordinates at time t=0 is the identity

mapping:

$$\tilde{\mathbf{x}} = \phi(\mathbf{X},0) = \mathbf{I}\cdot\tilde{\mathbf{X}} = \tilde{\mathbf{X}} \tag{50}$$

At any other instant of time, the motion is described by $\tilde{\mathbf{x}} = \phi\left(\tilde{\mathbf{X}},t\right)$. The displacement of a material point is given by the difference between its current position and its original position. This is expressed as:

$$\mathbf{u}\left(\tilde{\mathbf{X}},t\right) = \phi\left(\tilde{\mathbf{X}},t\right) - \phi\left(\tilde{\mathbf{X}},0\right) = \phi\left(\tilde{\mathbf{X}},t\right) - \tilde{\mathbf{X}} = \tilde{\mathbf{x}} - \tilde{\mathbf{X}} \tag{51}$$

An important variable in the description of body kinematics is the deformation gradient **F**. It is clear from the definition above that the deformation gradient can also be related to the displacements **u** in the following way:

$$\mathbf{F} = \frac{\partial\tilde{\mathbf{x}}}{\partial\tilde{\mathbf{X}}} = \frac{\partial\left(\mathbf{u}+\tilde{\mathbf{X}}\right)}{\partial\tilde{\mathbf{X}}} = \frac{\partial\mathbf{u}}{\partial\tilde{\mathbf{X}}} + \mathbf{I} \tag{52}$$

Where: **I** is the second order isotropic tensor.

In a Total Lagrangian formalism, the conservation of mass adopts the algebraic form given by Eq. (53) where: The Jacobian J is the determinant of the deformation gradient **F**.

$$J_0\rho_0 = J\rho \tag{53}$$

In the special case where the material and the spatial reference frames are coincident at time t=0 the Jacobian $J_0 = 1$ and consequently conservation of mass equation reduces to:

$$J^{-1}\rho_0 = \rho \tag{54}$$

The Momentum Equation in the Total Lagrangian formalism is given by:

$$\ddot{\mathbf{u}} = \frac{\mathbf{1}}{\rho_0}\nabla_{\mathbf{0}}\mathbf{P} + \mathbf{b} \tag{55}$$

Where: **P** is the nominal or the First Piola-Kirchhoff stress and **b** are the body forces per unit mass.

Finally, the conservation of energy is given by:

$$\dot{e} = \frac{\mathbf{1}}{\rho_0}\dot{\mathbf{F}} : \mathbf{P} \tag{56}$$

Where $\dot{e}$ is the rate of change of internal energy and $\dot{\mathbf{F}}$is the material velocity gradient.

To discretise Eq. (56) it is necessary to calculate $\dot{\mathbf{F}}$. This can be achieved by discretising Eq. (52) as:

$$\langle\mathbf{F}_I\rangle = -\sum_{J\in S}(\mathbf{u}_J - \mathbf{u}_I)\otimes\tilde{\nabla}_{\mathbf{0}}\tilde{W}_{IJ}\mathbf{V}_J^{\mathbf{0}} + \mathbf{I} \tag{57}$$

The velocity gradient used in Eq. (56) can be expressed as:

$$\left\langle\dot{\mathbf{F}}_I\right\rangle = -\sum_{J\in S}(\tilde{\mathbf{v}}_J - \tilde{\mathbf{v}}_I)\otimes\tilde{\nabla}_{\mathbf{0}}\tilde{W}_{IJ}\mathbf{V}_J^{\mathbf{0}} \tag{58}$$

In Eqs.(57) and (58) the symbol $\tilde{\nabla}_0$ represents the corrected approximation of the differential operator with respect to the material coordinates and $\mathbf{V_J^0}$ is the initial volume of particle $J$.

In order to calculate the stress rates using a rate form of a constitutive relation, it is necessary to determine the Green-Lagrange Strain Rate. Starting with the Green strain tensor expressed in terms of the gradient of deformation:

$$\mathbf{E} = \frac{\mathbf{1}}{\mathbf{2}}\left(\mathbf{F^T F} - \mathbf{I}\right) \tag{59}$$

And by taking the time derivative of Eq. (59) one gets the Green-Lagrange strain rate tensor which can be calculated using Eq. (57) and Eq. (58).

$$\dot{\mathbf{E}} = \frac{\mathbf{1}}{\mathbf{2}}\left(\dot{\mathbf{F}}^{\mathbf{T}}\mathbf{F} + \mathbf{F^T}\dot{\mathbf{F}}\right) \tag{60}$$

To integrate the constitutive equation, the Green-Lagrange strain rate tensor Eq. (60) is transformed into the rate of deformation tensor through the following expression:

$$\dot{\varepsilon} = \left(\mathbf{F}^{-T}\dot{\mathbf{E}}\mathbf{F}^{-1}\right) \tag{61}$$

The stress is integrated incrementally in time:

$$\begin{aligned}\sigma_{ij}(t+dt) &= \sigma_{ij}(t) + \dot{\sigma}_{ij}dt \\ &= \sigma_{ij}(t) + (\sigma_{ij}^{\nabla} + +\sigma_{ik}\omega_{kj} + \sigma_{jk}\omega_{ki})dt\end{aligned} \tag{62}$$

Where: the dot denotes the material derivative, ωis the spin tensor and $\sigma_{ij}^{\nabla} = C_{ijkl}\dot{\varepsilon}_{kl}$ is the Jaumann stress rate.

To integrate the conservation of momentum equation Cauchy stress is transformed into Nominal stress using the following transformation:

$$\mathbf{P} = \left(J\mathbf{F}^{-1}\sigma\right) \tag{63}$$

Eq. (63) is used to update accelerations in the conservation of momentum equation, Eq. (55).

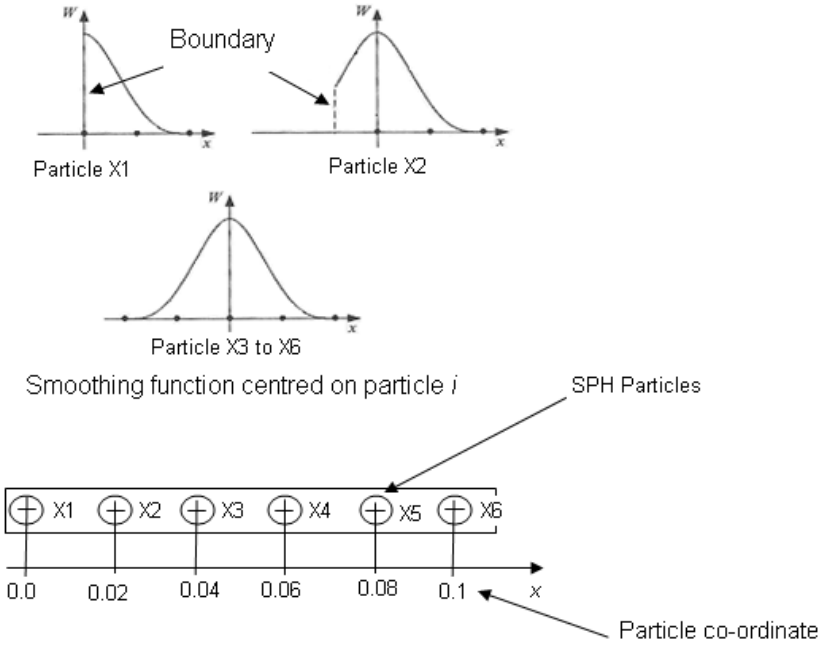


**Figure 1** : Schematic for Problem 1

### *4.2 Normalised-corrected Total Lagrangian interpolation.*

In the Total Lagrangian formalism the neighbourhood of particle $I$ remains fixed throughout the simulation. The interpolation correction used in this formalism is a direct extension of the correction methods developed for the ordinary SPH equations presented above.

The smoothing function is given in terms of the material coordinates $X$. Therefore the normalized kernel can be expressed as follows:

$$\tilde{W}\left(\tilde{\mathbf{X}}_J-\tilde{\mathbf{X}}_I,h\right)=\frac{W\left(\tilde{\mathbf{X}}_J-\tilde{\mathbf{X}}_I,h\right)}{\sum\limits_{J\in S}\frac{m_J}{\rho_J}W\left(\tilde{\mathbf{X}}_J-\vec{\mathbf{X}}_I,h\right)} \tag{64}$$

Since the denominator of the above expression remains constant, the derivative of the normalized kernel can be evaluated as:

$$\nabla\tilde{W}_{IJ}=\frac{1}{C}\nabla W_{IJ} \tag{65}$$

Where $C=\sum\limits_{J\in S}\frac{m_J}{\rho_J}W\left(\tilde{\mathbf{X}}_I-\tilde{\mathbf{X}}_J,h\right)$

The expression for the gradient correction term is given by:

$$\mathbf{B}=\left(-\sum_{J\in S}\frac{m_J}{\rho_J}\left(\tilde{\mathbf{X}}_J-\tilde{\mathbf{X}}_I\right)\otimes\nabla\tilde{W}\right)^{-1} \tag{66}$$

The gradient correction $\mathbf{B}$ operates over the gradient of the smoothing function according to Eq. (48). Hence, the final expression for the corrected gradient of deformation, in a Total Lagrangian framework is:

$$\langle\mathbf{F}_I\rangle=\left(-\sum_{J\in S}(\mathbf{u_J}-\mathbf{u_I})\otimes\nabla_{\mathbf{0}}\tilde{W}_{\mathbf{IJ}}\mathbf{V_J^0}\right)\mathbf{B}+\mathbf{I} \tag{67}$$

The corrected momentum equation is:

$$\langle\mathbf{a}_I\rangle=\left(-\sum_{J\in S}(\mathbf{P_J}-\mathbf{P_I})\otimes\nabla_{\mathbf{0}}\tilde{W}_{\mathbf{IJ}}\mathbf{V_J^0}\right):\mathbf{B} \tag{68}$$

and the corrected conservation of energy equation is expresses as

$$\langle\dot{e}_I\rangle=\mathbf{P}_J:\left[\left(-\sum_{J\in S}\frac{m_J}{\rho_I\rho_J}(\mathbf{v}_J-\mathbf{v}_I)\otimes\nabla_0\tilde{W}_{IJ}\mathbf{V}_J^0\right)\mathbf{B}\right] \tag{69}$$

The Total Lagrangian corrected equations are much simpler for numerical implementation than their Eulerian corrected SPH counterparts. Few examples are given in the following section.

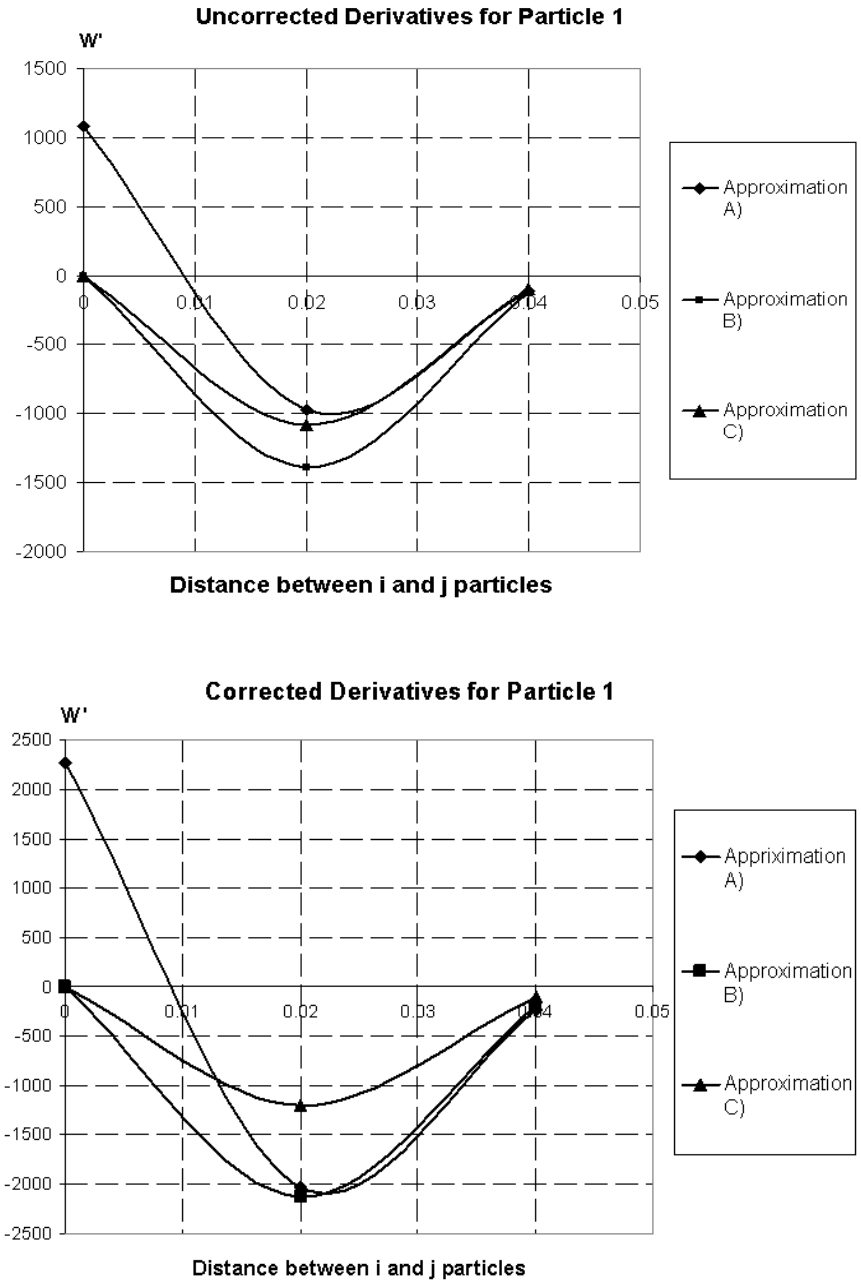


**Figure 2** : Kernel derivative estimates for particle X1

## 5 Numerical Examples.

### *5.1 Approximation of constant and linear velocity fields*

Consider the following set of discrete points in 1-D and their associated value of velocity as shown in Tab. 2. We would like to evaluate the approximation of the velocity gradient at every point using conventional SPH, normalized-corrected SPH and Total Lagrangian normalized-corrected SPH.

*Results.*

The advantages of the Total Lagrangian normalized corrected code become evident in this simple example. Fig. 2, 3 and 4 show the uncorrected and corrected values of the derivatives for two particles with incomplete support (Particles 1 and 2) and a particle with complete support (Particle 3). The resulting values for the velocity gradient approximation can be found in Tab. 3 and 4 in Appendix

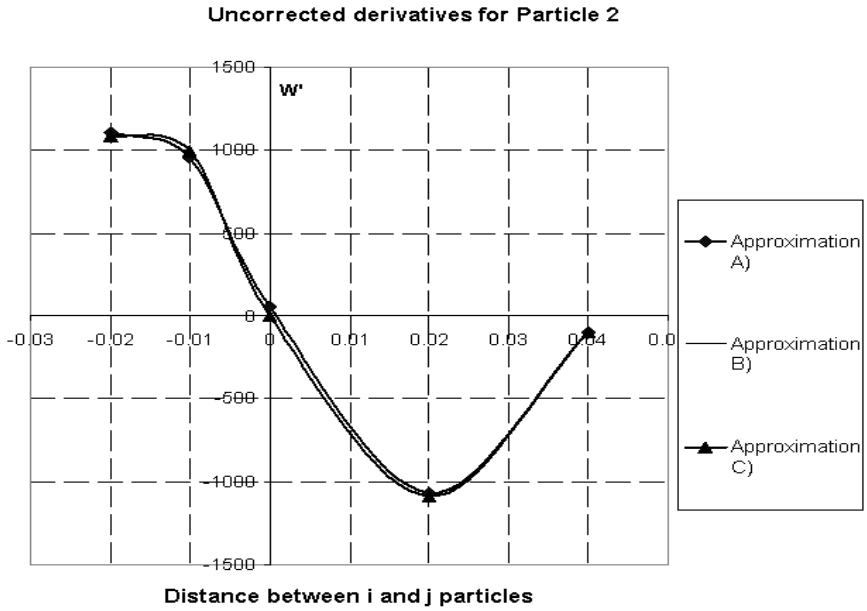


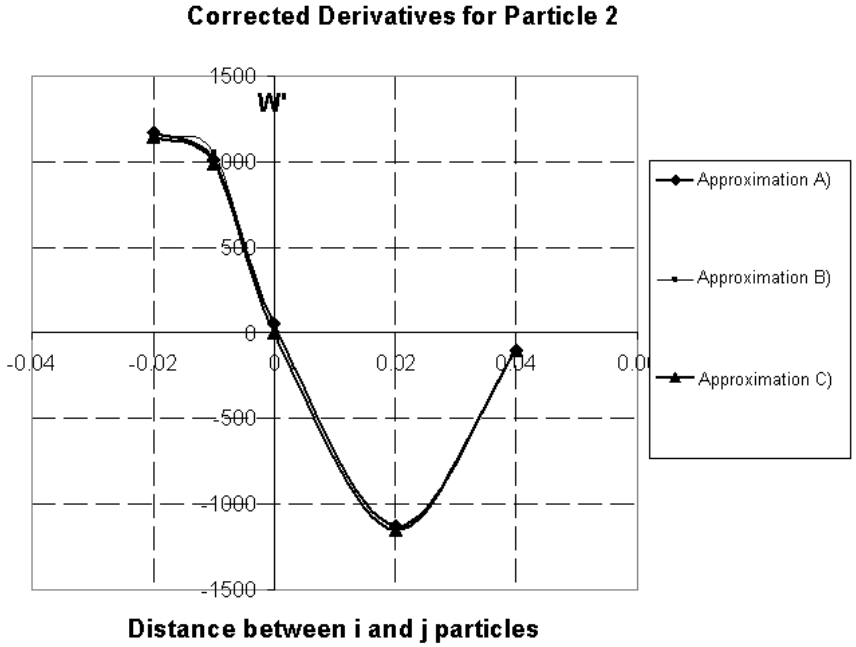


**Figure 3** : Kernel derivative estimates for particle X2

A.

Tab. 4 shows the approximation of a linear velocity field using three SPH schemes and the effect of symmetrisation over the approximation. Ordinary SPH (Approximation C) is incapable of approximating the derivative neither with nor without symmetrisation in the interpolating equation. The Total Lagrangian scheme (Approximation B) can approximate the gradient only if the symmetrisation term is present in the equation whereas the scheme suggested by Vignjevic, Campbell and Libersky (2000), Bonet and Kulasegaram (2002) and Bonet, Kulasegaram, Rodriguez-Paz and Profit (2004) (Approximation A) re-

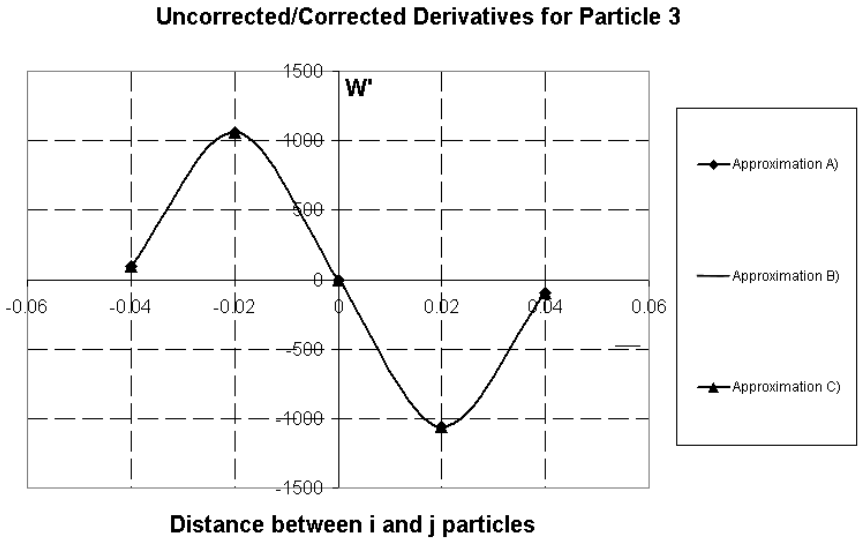


**Figure 4** : Kernel derivative estimates for particle X3 to X6

**Table 2** :

| Particle Number | Velocity Field | |
|---|---|---|
| | Linear | Constant |
| X1 | -0.04 | 0.002 |
| X2 | -0.06 | 0.002 |
| X3 | -0.08 | 0.002 |
| X4 | -0.1 | 0.002 |
| X5 | -0.12 | 0.002 |
| X6 | -0.14 | 0.002 |

quires no symmetrisation for the approximation of the derivatives.

Tab. 3 provides the results for the approximation of a constant velocity field. All schemes can easily handle this problem, they all work well when the symmetrisation term is present and only one of them (Approximation A) provides accurate results when the symmetry term gets removed.

### *5.2 Simulation of Titanium and Aluminium plate impact test .*

The capabilities of the Total Lagrangian normalized-corrected SPH are demonstrated on this 2-D example.

The materials under consideration are Aluminium as the target plate and Titanium as the flyer plate.

The plates are modelled using the elastic-perfectly plastic material model. The initial velocity of the flyer is $550.00 m s^{-1}$. The material properties are as follows: Titanium; density$4530.00\,Kg\,m^{-3}$, mass $0.0442Kg$, Young modulus 1.16E05 *MPa*, Poisson ration 0.342, Aluminium; density$2780.00\,Kg\,m^{-3}$, mass $0.112Kg$, Young modulus 0.743E05 *MPa,* Poisson ratio 0.342. The SPH model is discretised in 5000 particles.

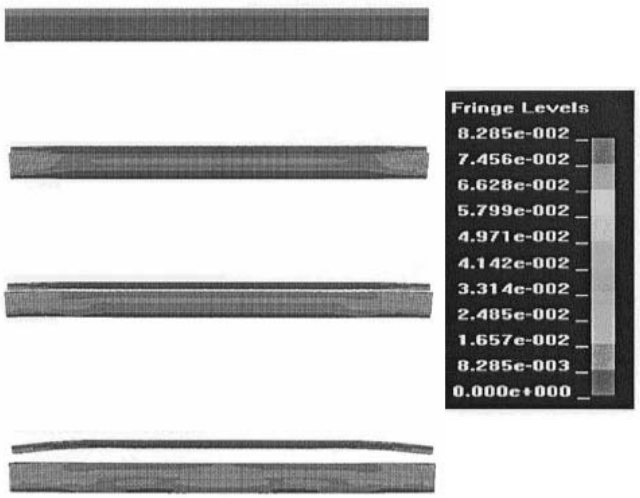


**Figure 5** : Two plate impact sequence, Effective Plastic strain shown.

*Results.*

The results shown in Fig. 5 show the impact sequence of the two plates and the resulting contours of effective plastic strain. The type of contact algorithm used is described in T. De Vuyst, R. Vignjevic, J. Campbell (2005). The type of correction used in the SPH code is denoted

**Table 3** : Constant velocity field approximation.

| | | | | |
|---|---|---|---|---|
| Method A) | $\nabla \widetilde{W} = \frac{\nabla W * \sum WV - W \sum \nabla WV}{\sum WV^2}$ | | | |
| Mehotd B) | $\nabla \widetilde{W} = \frac{1}{\sum WV} * \nabla W$ | | | |
| Method C) | $\nabla \quad W$ | | | |
| i Particle | With respect to particle | Corrected Derivative Value | | |
| | | Method A) | Method B) | Method C) |
| Particle 1 | X2-X1 | -2024.0987 | -2122.5335 | -1085.0600 |
| | X3-X1 | -237.8687 | -188.6016 | -96.4500 |
| | X1-X1 | 2262.0091 | 0.0000 | 0.0000 |
| Particle 2 | X1-X2 | 1170.7575 | 1147.9624 | 1085.0600 |
| | X2-X2 | 56.8991 | 0.0000 | 0.0000 |
| | X3-X2 | -1126.1052 | -1147.9624 | -1085.0600 |
| | X4-X2 | -101.5514 | -102.0376 | -96.4500 |
| Particle 3 | X1-X3 | 94.3253 | 94.3321 | 96.4500 |
| | X2-X3 | 1061.8778 | 1061.8778 | 1085.0600 |
| | X3-X3 | 0.0000 | 0.0000 | 0.0000 |
| | X4-X3 | -1061.8778 | -1061.8778 | -1085.0600 |
| | X5-X3 | -94.3253 | -94.3253 | -96.4500 |
| Approximation of $\frac{\partial v}{\partial x}$ with no symmetrisation terms: $\nabla v_i = -\sum_{j \in S} \frac{m_j}{\rho_j} v_j \nabla W_{ij}$ | | | | |
| Using Method A) | Approximation for Particle 1: | 0.0000 | | |
| | Approximation for Particle 2: | 0.0000 | | |
| | Approximation for Particle 3: | 0.0000 | | |
| Using Method B) | Approximation for Particle 1: | 0.0924 | | |
| | Approximation for Particle 2: | 0.0041 | | |
| | Approximation for Particle 3: | 0.0000 | | |
| Using Method C) | Approximation for Particle 1: | 0.0473 | | |
| | Approximation for Particle 2: | 0.0039 | | |
| | Approximation for Particle 3: | 0.0000 | | |
| Approximation of $\frac{\partial v}{\partial x}$ with symmetrisation terms: $\nabla v_i = -\sum_{j \in S} \frac{m_j}{\rho_j} (v_j - v_i) \nabla W_{ij}$ | | | | |
| Using Method A) | Approximation for Particle 1: | 0.0000 | | |
| | Approximation for Particle 2: | 0.0000 | | |
| | Approximation for Particle 3: | 0.0000 | | |
| Using Method B) | Approximation for Particle 1: | 0.0000 | | |
| | Approximation for Particle 2: | 0.0000 | | |
| | Approximation for Particle 3: | 0.0000 | | |
| Using Method C) | Approximation for Particle 1: | 0.0000 | | |
| | Approximation for Particle 2: | 0.0000 | | |
| | Approximation for Particle 3: | 0.0000 | | |

**Table 4** : Linear velocity field approximation.

| | | | | |
|---|---|---|---|---|
| Method A) | $\nabla \widetilde{W} = \frac{\nabla W * \sum WV - W \sum \nabla WV}{\sum WV^2}$ | | | |
| Mehotd B) | $\nabla \widetilde{W} = \frac{1}{\sum WV} * \nabla W$ | | | |
| Method C) | $\nabla \quad W$ | | | |
| i Particle | With respect to particle | Corrected Derivative Value | | |
| | | Method A) | Method B) | Method C) |
| Particle 1 | X2-X1 | -2024.0987 | -2122.5335 | -1085.0600 |
| | X3-X1 | -237.8687 | -188.6016 | -96.4500 |
| | X1-X1 | 2262.0091 | 0.0000 | 0.0000 |
| Particle 2 | X1-X2 | 1170.7575 | 1147.9624 | 1085.0600 |
| | X2-X2 | 56.8991 | 0.0000 | 0.0000 |
| | X3-X2 | -1126.1052 | -1147.9624 | -1085.0600 |
| | X4-X2 | -101.5514 | -102.0376 | -96.4500 |
| Particle 3 | X1-X3 | 94.3253 | 94.3321 | 96.4500 |
| | X2-X3 | 1061.8778 | 1061.8778 | 1085.0600 |
| | X3-X3 | 0.0000 | 0.0000 | 0.0000 |
| | X4-X3 | -1061.8778 | -1061.8778 | -1085.0600 |
| | X5-X3 | -94.3253 | -94.3253 | -96.4500 |
| Approximation of $\frac{\partial v}{\partial x}$ with no symmetrisation terms: $\nabla v_i = -\sum_{j \in S} \frac{m_j}{\rho_j} v_j \nabla W_{ij}$ | | | | |
| Using Method A) | Approximation for Particle 1: | -0.9999 | | |
| | Approximation for Particle 2: | -0.9999 | | |
| | Approximation for Particle 3: | -1.0004 | | |
| Using Method B) | Approximation for Particle 1: | -2.8488 | | |
| | Approximation for Particle 2: | -1.1224 | | |
| | Approximation for Particle 3: | -0.9999 | | |
| Using Method C) | Approximation for Particle 1: | -1.4564 | | |
| | Approximation for Particle 2: | -1.0610 | | |
| | Approximation for Particle 3: | -1.0224 | | |
| Approximation of $\frac{\partial v}{\partial x}$ with symmetrisation terms: $\nabla v_i = -\sum_{j \in S} \frac{m_j}{\rho_j} (v_j - v_i) \nabla W_{ij}$ | | | | |
| Using Method A) | Approximation for Particle 1: | -0.9999 | | |
| | Approximation for Particle 2: | -0.9999 | | |
| | Approximation for Particle 3: | -1.0004 | | |
| Using Method B) | Approximation for Particle 1: | -0.9999 | | |
| | Approximation for Particle 2: | -1.0000 | | |
| | Approximation for Particle 3: | -1.0004 | | |
| Using Method C) | Approximation for Particle 1: | -0.5112 | | |
| | Approximation for Particle 2: | -0.9452 | | |
| | Approximation for Particle 3: | -1.0224 | | |

by B) in Problem 1 since this scheme proved to be computationally efficient and numerically accurate. The corrected SPH equations employed for this simulation are supplied in section 4.2 of this document.

### 5.3 Normal Impact.

This problem illustrates the normal impact of a prismatic projectile on a square, 0.30 x 0.30 $m$ Al7010T7651 plate, with an 0.011 $m$ thickness. The projectile velocity is 137.00 $ms^{-1}$, 0.74 $Kg$ weight and is characterised as linear elastic. The material model employed to simulate the behaviour of the target plate is the Johnson Cook Model with damage. The behaviour is described through the Johnson-Cook model:

$$\sigma_{yield} = (A + B\bar{\varepsilon}^{p^n})(1 + C\ln(\dot{\varepsilon}^*))\,[1 - (T^*)^m] \tag{70}$$

where $A$, $B$, $C$, $n$, and $m$ are input constants and the temperature $T^*$ is the homologous temperature which is raised to the power $m$ in Eq. (70), this is given by:

$$T^* = \frac{T - T_{room}}{T_{melt} - T_{room}} \tag{71}$$

The Johnson-Cook model also includes damage parameters that enable element or particle deletion at a specified effective plastic strain

$$\varepsilon_f = [D_1 + D_2 \exp(D_3\sigma^*)]\,[1 + D_4 \ln(\dot{\varepsilon}^*)]\,[1 + D_5 T^*] \tag{72}$$

where $\varepsilon_f$is the strain at failure, $D_1 - -D_5$ are the failure parameters and $\sigma^*$ is the ratio of pressure divided by the effective stress:

$$\sigma^* = \frac{P}{\overline{\sigma}} \tag{73}$$

where effective stress $\overline{\sigma}$is found from:

$$\overline{\sigma} = \sqrt{\frac{3}{2} S_{ij} S_{ij}} \tag{74}$$

Fracture occurs when the damage parameter,

$$D = \sum \frac{\Delta\bar{\varepsilon}^p}{\varepsilon_f} \tag{75}$$

reaches the value of 1.

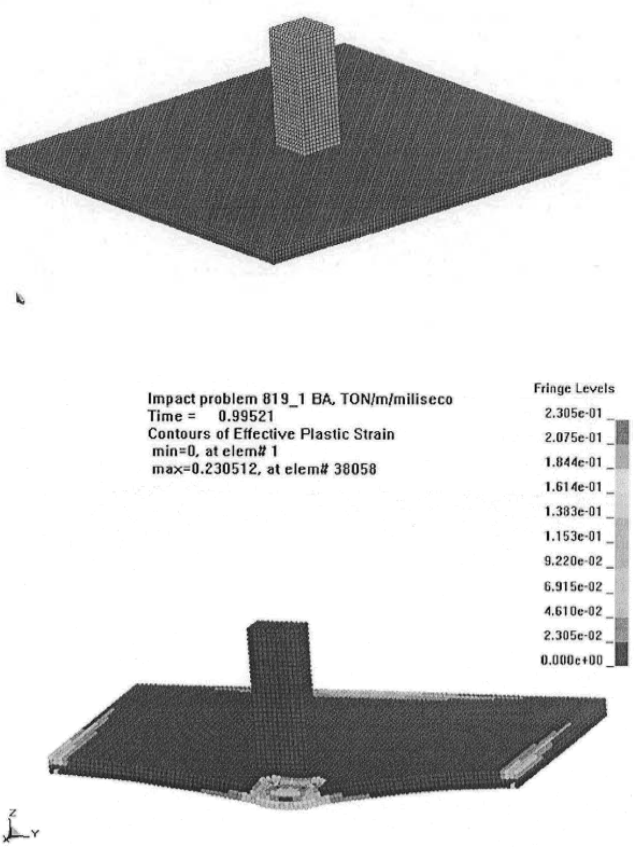


**Figure 6** : SPH discretisation and effective plastic strain for normal plate impact

The Johnson-Cook model requires an equation of state to be specified. Two equations of state have been considered in this paper. The linear polynomial equation of state was used to characterise the behaviour of the target plate. The polynomial equation of state is given as follows:

$$P = C_0 + C_1\mu + C_2\overline{\mu}^2 + C_3\mu^3 + + \left(C_4 + C_5\mu + C_6\overline{\mu}^2\right) E \tag{76}$$

where $E$ is the internal energy, $C_0 - -C_6$ are coefficients with $C_1$ being the bulk modulus, and the excess compression $\mu$ is:

$$\mu = \frac{\rho}{\rho_0} - 1 \tag{77}$$

with $\rho_0$ as the initial material density.

*Results.*

Fig. 6 shows the results of the simulation using the Total Lagrangian SPH code. The plots presented in Fig. 7

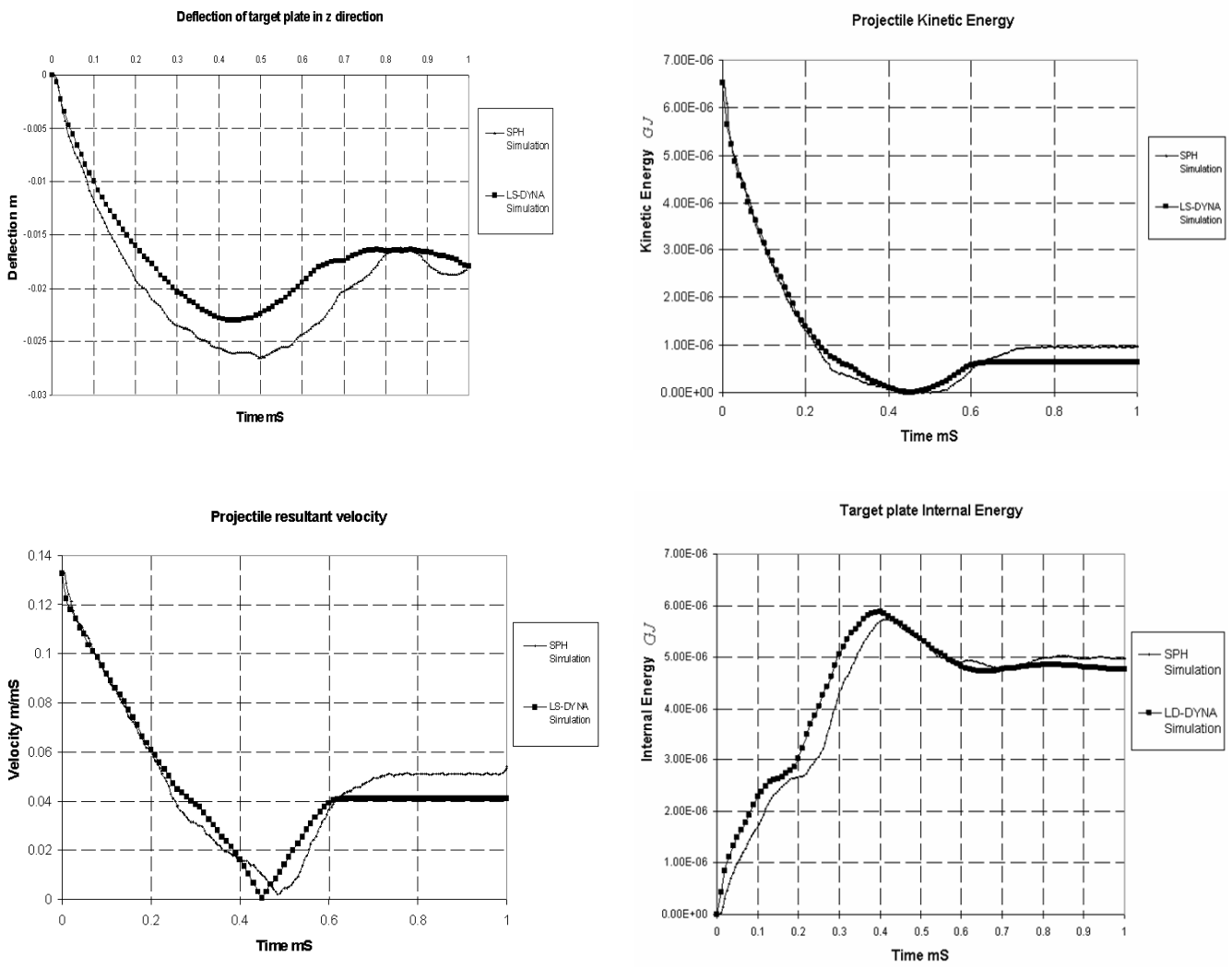


**Figure 7** : LS-DYNA vs Total Lagrangian SPH results for normal impact.

show how the SPH and FE results compare. The SPH results are remarkably similar to the FE results, but discrepancies were observed for the total deflection of the plate in the direction of impact. This can be easily explained due to the fact that only four SPH particles were defined through the plate thickness. The more refined LS-DYNA model employs a finer discretisation through the plate thickness (10 solid elements). Nevertheless, the maximum error observed in the value of deflection is about 18% and the source of error can be attributed to a coarser SPH discretisation which can be straightforwardly corrected.

### *5.4 Spall fracture simulation of OFHC Copper using total Lagrangian SPH and Johnson-Cook with damage.*

In this example, spall fracture was simulated using a 3-D arrangement of 9375 SPH particles as shown in Fig. 8. Symmetry planes were imposed to ensure a one dimensional state of strain across the plate thickness. The thickness ratio between flyer and target plates is 1:2 which allows us to easily verify the location of spall within the target plate when fracture occurs.

Two cases were simulated. In the first case, the flyer plate impacts the target with a $290.00 ms^{-1}$ velocity. In the second case, the flyer travels at $305.00 ms^{-1}$ . A particle-to-particle contact algorithm was used to simulate the interaction of the two plates and details can be found in

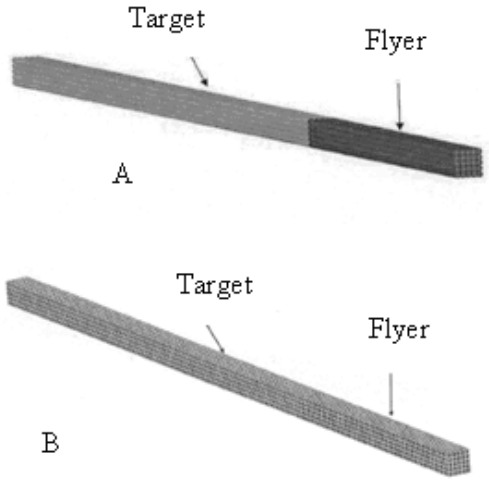


**Figure 8** : Spall fracture simulation: A)SPH discretisation, B) Finite Element discretisation.

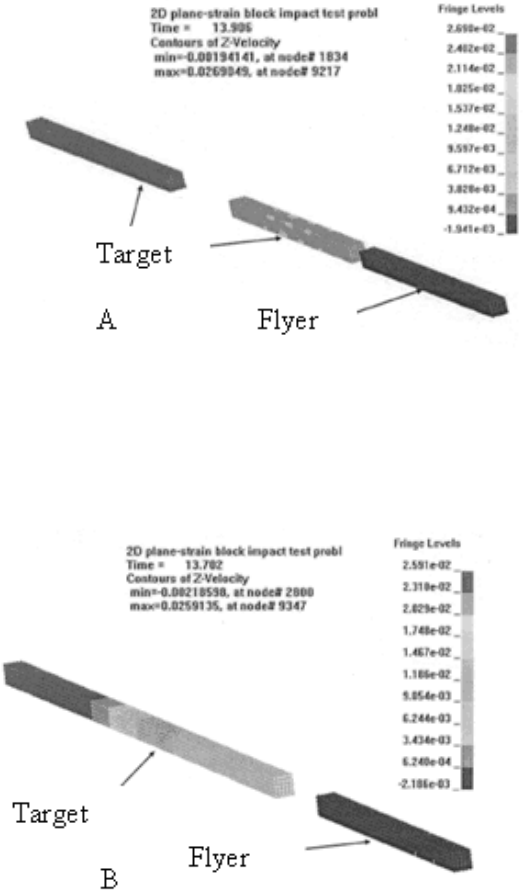


**Figure 9** : Two plate impact scenarios in SPH: A) Spallation occurs, impact velocity $305.00 m s^{-1}$. B) No spallation occurs, impact velocity $290.00 m s^{-1}$

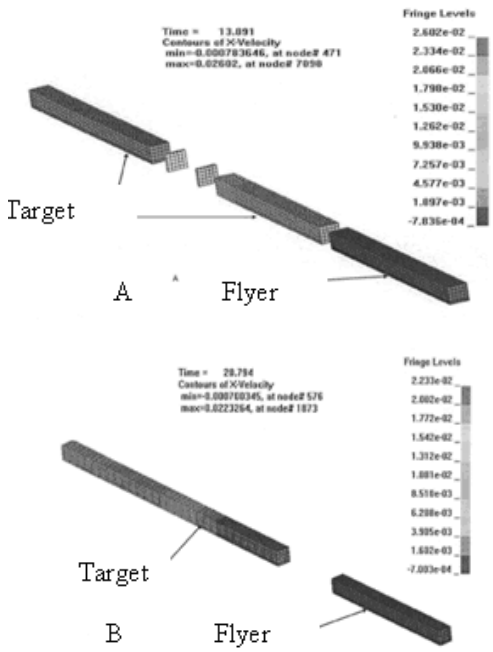


**Figure 10** : Two plate impact scenarios in FE: A) Spallation occurs, impact velocity $305.00 m s^{-1}$. B) No spallation occurs, impact velocity $290.00 m s^{-1}$.

De Vuyst, Vignjevic and Campbell (2005). The Johnson-Cook model together with the Gruneisen equation of state, was used to characterize the two copper plates. The Gruneisen equation of state with cubic shock velocity-particle velocity defines pressure for a compressed material as:

$$P = \frac{\rho_0 C_0^2 \mu \left[1 + \left(1 - \frac{\gamma_0}{2}\right)\mu - \frac{a}{2}\mu^2\right]}{\left[1 - (S_1 - 1)\mu - S_2 \frac{\mu^2}{\mu+1} - S_3 \frac{\mu^3}{(\mu+1)^2}\right]^2} + (\gamma_0 + a\mu) E \tag{78}$$

where $C_0$ is the is the intercept of the $u_s - u_p$ curve $S_1, S_2$ and $S_3$ are the coefficients of the slopes of the $u_s - u_p$ curve, $\gamma_0$is the Gruneisen gamma, and $a$ is the first order volume correction to $\gamma_0$, $\mu$ as defined in the previous example.

For expanded materials the pressure is defined as:

$$P = \rho_0 C_0^2 \mu + (\gamma_0 + a\mu) E \tag{79}$$

The damage parameters $D_i$ required by the Johnson-Cook with damage model were obtained from V. Ikkurthi, S. Chaturvedi (2004) and are as follows: $D_1 =$

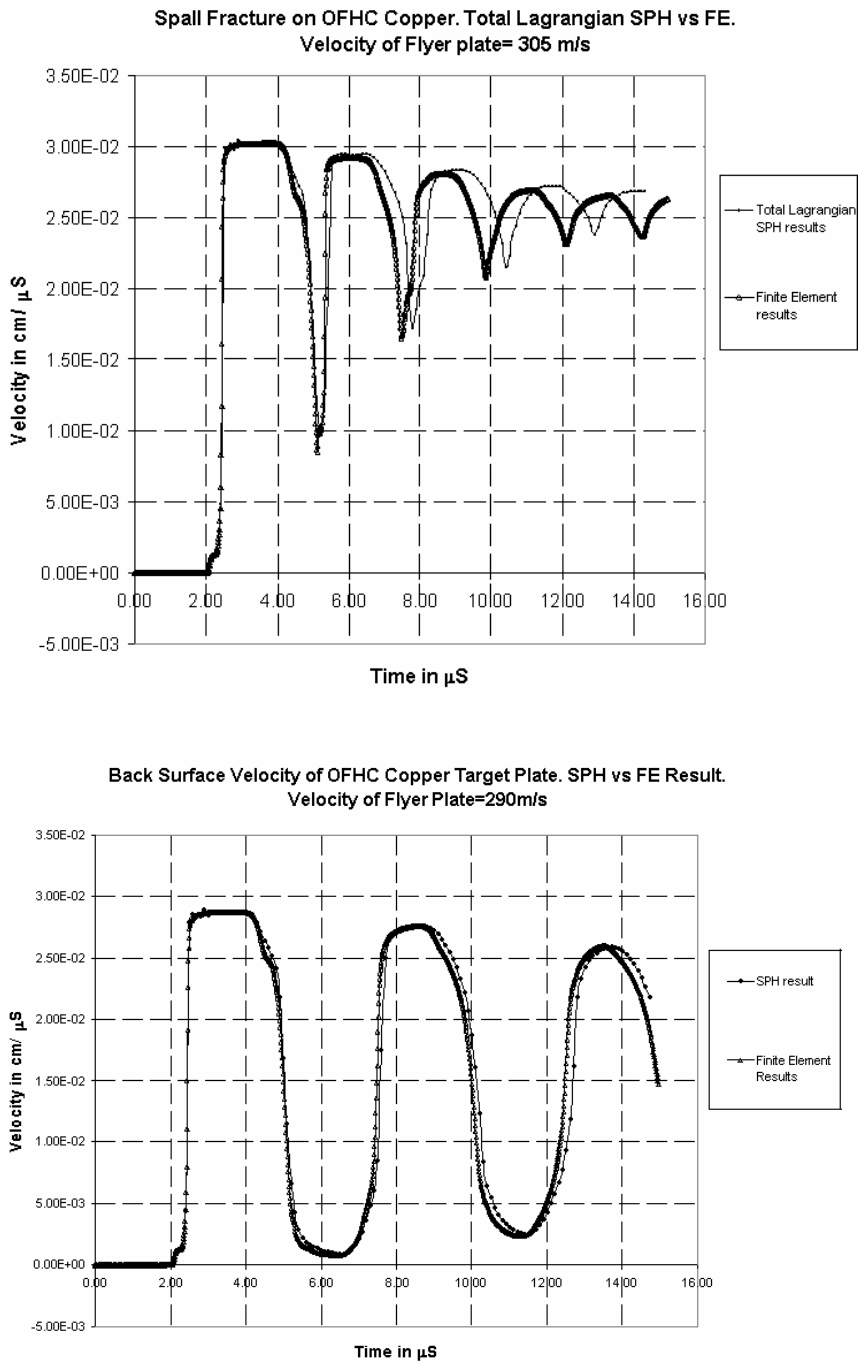


**Figure 11** : Target plate back surface velocity plot. Simulations show Total Lagrangian SPH vs Finite Element results.

0.54, $D_2 = 4.89$, $D_3 = -3.03$, $D_4 = 0.014$, and we set $D_5 = 0.0$

The value of the constants required were obtained from D. Steinberg (1996) for OFHC Copper:$A = 90.00 MPa$, $B = 292.00 MPa$, $C = 0.025$, $n = 0.31$, $m = 1.09$. The values for the shear modulus $G$,the density ρ and the value for the specific heat $c_v$ were also obtained from D. Steinberg (1996): 47.70$GPa$, 8960.00 $Kgm^{-3}$ and 383.00$JKg^{-1}K^{-1}$respectively.

The Gruneisen equation of state constants were obtained

from D. Steinberg (1996) for OFHC Copper: $C_o = 3940.00 m\,s^{-1}$, $S_1 = 1.489$, $S_2 = 0.0$, $S_3 = 0.0$, $\gamma_0 = 2.02$ and $b = 0.47$.

*Results.*

The results of this simulation are presented in Fig. 9, 10 and 11. Two possible outcomes of the SPH simulation are presented in Fig. 9, where the formation of a spall layer within the domain is dependant upon the impact velocity of the flyer. The localization of the spall layer can be verified by simple inspection. Since the thickness ratio between the flyer and the target plate is 1:2, it is expected that fracture within the target will occur where reflected rarefaction waves produce a state of high tension (i.e. halfway through the target plate). The SPH simulations demonstrate that even in zones of high tensile stresses, numerical fracture is avoided by the superior stability qualities of the Total Lagrangian scheme (Refer to Fig. 9, B). Consequently, only real fracture is visualized in the specimen (Fig. 9, A). Fig. 10 replicates the same scenarios with conventional FE. The localization of the spall fracture is equivalent to that in SPH. The resulting target plate back surface velocity is presented in Fig. 11. The correlation between SPH and FE results is remarkable during both, spall (velocity =305 $ms^{-1}$) and no spall (velocity=290 $ms^{-1}$) scenarios.

## 6 Conclusions

The effectiveness of the total Lagrangian SPH approach and the normalization and correction terms introduced was demonstrated in the examples presented here. The results suggest that this technique is just as accurate as its ordinary SPH counterpart when symmetrisation terms are considered in the discretised equations. A full derivation of the mixed interpolation correction based on Noether's theorem was presented. This correction ensures that homogeneity and isotropy of space are preserved in the process of spatial discretisation. Consequently, conservation of linear and angular momentum is ensured. The corrections introduced render the method $1^{st}$ order consistent and the normalization of the smoothing function ensures the particle deficiency problem at the boundaries gets corrected. A clear advantage of the Normalised-Corrected Total Lagrangian SPH method becomes evident when this technique is introduced in a numerical code since this approach is much easier for implementation and computationally less expensive than the ordinary normalized-corrected technique.

## References

**Atluri, S.N., and Zhu, T** (1998): A New Meshless Local Petrov-Galerkin (MLPG) Approach in Computational Mechanics, *Computational Mechanics*, Vol.22, pp. 117-127.

**Atluri SN, Han ZD, Rajendran AM**(2004): A new implementation of the meshless finite volume method, through the MLPG "Mixed" approach, *CMES: Computer Modeling in Engineering & Sciences*, Vol.6, No. 6, pp. 491-513.

**Z. D. Han; A. M. Rajendran; and S.N. Atluri** (2005):Meshless Local Petrov-Galerkin (MLPG) Approaches for Solving Nonlinear Problems with Large Deformations and Rotations, *CMES: Computer Modeling in Engineering & Sciences*, Vol. 10, No. 1, pp. 1-12

**Bonet, J.; Kulasegaram, S.** (2000): Correction and Stabilisation of Smooth Particle Hydrodynamics methods with applications metal forming simulation, *Int. Jour. Num. Mehtods . Enginr.* V.47, pp.1189-1214

**Bonet, J.; Kulasegaram, S.** (2002): A Simplified Approach to Enhance the Performance of Smooth Particle Hydrodynamics, *Comput. Methods Appl. Mech. Eng*, V. 126, pp.133-155

**Bonet, J.; Kulasegaram, S.; Rodriguez-Paz,M. M. X**. (2004): Profit, Variational Formulation for the Smooth Particle Hydrodynamics (SPH) simulation of fluid and solid problems, *Computer Methods in Applied Mechanics and Engineering*, V.193, pp. 1245-1256

**De Vuyst, T.; Vignjevic, R.; Campbell, J**. (2005): Coupling between meshless and finite element methods, *International Journal of Impact Engineering*, V.31, pp.1054-1064

**Dyka, C.; Ingel, R. P.** (1995): An Approach for tension instability in Smoothed Particle Hydrodynamics, *Computers and Structures*, V.59, pp. 573-580

**Gelfand, I. M.; Fomin, S. V.** (1963): Calculus of Variations, Prentice-Hall Inc., pp.79-83, 177-179

**Gingold, R A.; Monaghan, J. J**. (1977): Smoothed Particle Hydrodynamics: Theory and application to non-spherical stars, *Mon. No. Royal Astronomical Society*, 181,375

**Ikkurthi, V. R.; Chaturvedi, S.** (2004): Use of different damage models for simulating impact-driven spallation in metal plates, *International Journal of Impact Engineering*, V.30, pp.275-301

**Johnson, G. R.; Stryk, R. A.; Beissel, S. R.** (1996): SPH for high velocity computations, *Comput. Methods Appl. Mech. Eng*, V. 139, pp. 347-373

**Liu, W. K.; Chen, Y**. (1995): Wavelet and Multiple – scale reproducing kernel methods, *International Journal for Numerical Methods in Fluids*, V.21,pp.901-931

**Liu, W.; Jun, S.; Adee, J.; Belytschko, T.** (1995): Reproducing kernel particle methods for structural dynamics, *Int. J.Numer.Meth.Eng*, 38

**Lucy, L. B**. (1977): A Numerical Approach to the Testing of the Fission Hypothesis, Astron. J.82,1013**Monaghan, J. J.** (1992): *Smoothed Particle Hydrodynamics*, *Annual Rev. Astron.Astrophys*, pp. 543-574

**Rabczuk, T.; Belytschko, T.; Xiao, S. P.** (2004): Stable particle methods based on Lagrangian kernels. *Comput. Methods Appl. Mech. Eng*, V. 193, Issues 12-14, pp. 1035-1063

**Randles, P. W.; Libersky, L. D**.(1996): Smoothed Particle Hydrodynamics: Some recent improvements and applications, *Comput. Methods Appl. Mech. Eng* V. 139: pp. 375-408

**Steinberg, D. J.** (1996): Equation of state and strength properties of selected materials, LLNL

**Sweegle, J. W.; Hicks, D. L.; Attaway, S. W**. (1995): Smoothed Particle Hydrodynamics Stability Analysis, *J.Comp. Physics*, V.116,pp.123-134

**Vignjevic, R.; Campbell, J.; Libersky, L.** (2000): A treatment of zero-energy modes in the smoothed particle hydrodynamics method, *Comput. Methods Appl. Mech. Eng*, V. 184, pp. 67-85